

NJC

Accepted Manuscript



This is an *Accepted Manuscript*, which has been through the Royal Society of Chemistry peer review process and has been accepted for publication.

Accepted Manuscripts are published online shortly after acceptance, before technical editing, formatting and proof reading. Using this free service, authors can make their results available to the community, in citable form, before we publish the edited article. We will replace this *Accepted Manuscript* with the edited and formatted *Advance Article* as soon as it is available.

You can find more information about *Accepted Manuscripts* in the [Information for Authors](#).

Please note that technical editing may introduce minor changes to the text and/or graphics, which may alter content. The journal's standard [Terms & Conditions](#) and the [Ethical guidelines](#) still apply. In no event shall the Royal Society of Chemistry be held responsible for any errors or omissions in this *Accepted Manuscript* or any consequences arising from the use of any information it contains.



www.rsc.org/njc

Conformational Insights and Vibrational Study of a Promising Anticancer
Agent:
The Role of the Ligand in Pd(II)-Amine Complexes

Sónia M. Fiuza^{*a}, Ana M. Amado^a, Stewart F. Parker^b, Maria Paula M. Marques^{a,c} and
Luís A. E. Batista de Carvalho^a

^a*Unidade de I&D “Química-Física Molecular”, Departamento de Química, Universidade de Coimbra,
P-3004 535 Coimbra, Portugal.*

^b*ISIS Facility, STFC Rutherford Appleton Laboratory, Chilton, Didcot, OX 11 0QX, United Kingdom*

^c*Departamento de Ciências da Vida, P-3000 456, Universidade de Coimbra, Coimbra, Portugal*

*Correspondence author:
Tel./Fax: +351-239 826541
email: sonia.mfiuza@gmail.com

Abstract

A conformational and vibrational analysis of an antiproliferative spermine-based dinuclear Pd(II) complex (Pd₂-Spm) is reported. Density Functional Theory coupled to all-electron basis sets was used to perform quantum mechanical calculations, aiming at determining the best suited strategy for accurately representing this molecule, and achieve an optimal accordance with the experimental data. The structural parameters and the vibrational frequencies predicted by the calculations are compared with the corresponding experimental data. The results support a relationship between the strength of the metal-ligand bonds and the antitumor activity of the compound.

Keywords

palladium(II); spermine; metal-ligand bond; anticancer; vibrational spectroscopy; quantum mechanical calculations

1. INTRODUCTION

Palladium(II) complexes are an emerging class of inorganic compounds bearing recognized anticancer properties,¹⁻⁵ challenging the initial belief that complexes containing this metal centre would be inactive. This conviction started to materialize with the lack of biological activity of their parent compound *cis*-diamminedichloropalladium(II) (cDDPd),⁶ as opposed to its Pt(II) homologue (cisplatin, *cis*-diamminedichloroplatinum(II), cDDP) that was justified by the higher lability of palladium(II) complexes relative to the platinum(II) ones. However, this problem has been circumvented by different synthetic strategies, most of them aiming at lowering this kinetic lability by coordination of the metal to polydentate or bulky ligands, yielding compounds with interesting therapeutic properties, largely determined by the nature of the ligands.⁷⁻¹² Kovala-Demertzi and co-workers¹³ published an interesting study in which the substitution of a hydrogen for a methyl group in a bulky ligand has turned a biologically inactive compound into an active one. This shows that there is still much to be understood at the molecular level to unveil the physico-chemical phenomena that rule the behaviour of these metal-based compounds in living systems – their structure-activity relationships (SAR's) being of paramount importance. Pd(II) complexes are particularly interesting compounds to perform SAR's studies, as the effect of the ligand on their biological activity is generally more pronounced than for their Pt(II) counterparts.

The present study focuses on a polynuclear Pd(II) chelate with a biogenic polyamine (spermine) – $\{\mu\text{-}\{N,N'\text{-bis}[(3\text{-amino-}\kappa N)\text{propyl}]butane\text{-}1,4\text{-diamine-}\kappa N:\kappa N'\}\}$ tetrachloro-dipalladium (II), Pd₂-Spm (Figure 1.A).¹⁴

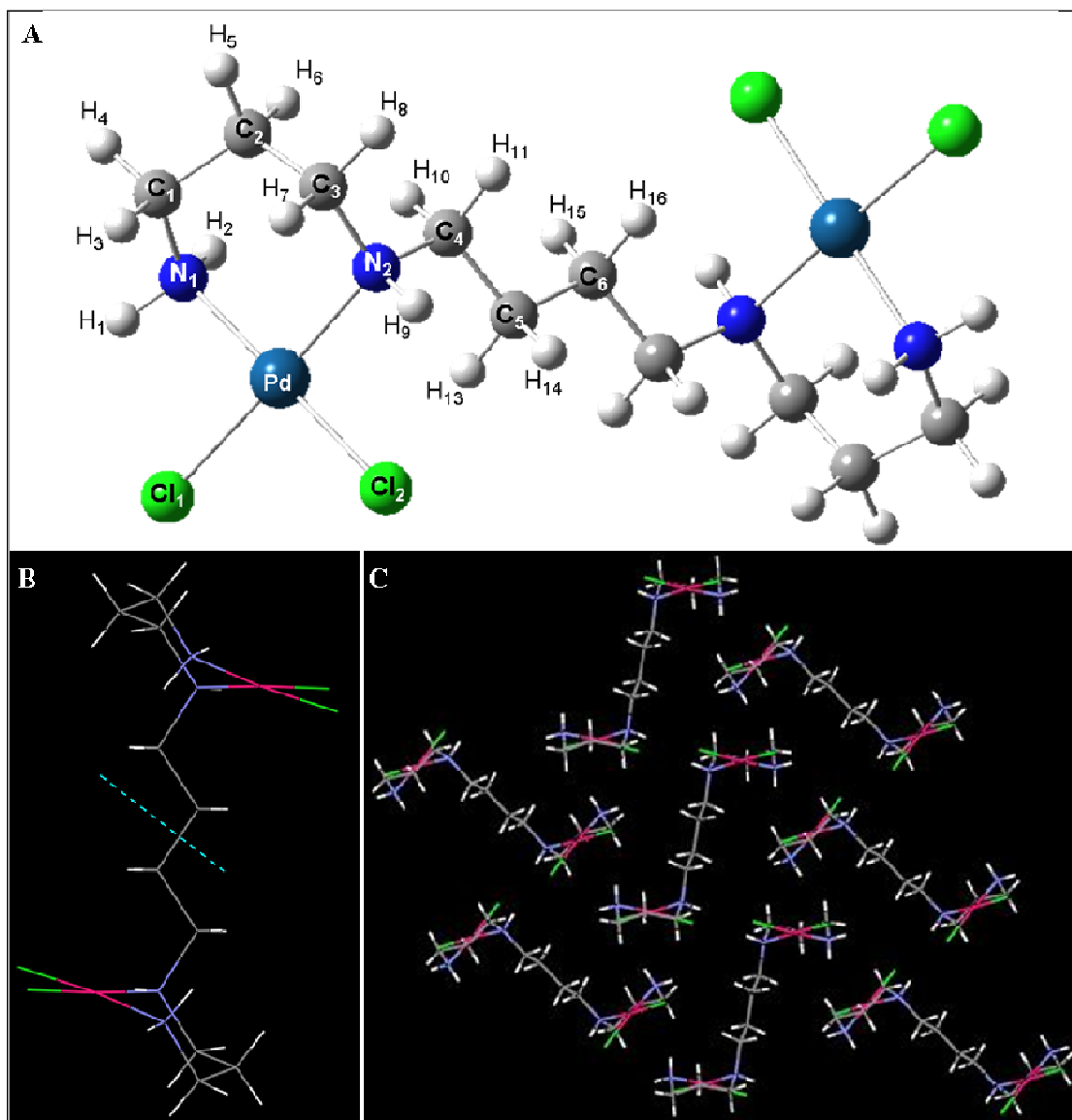


Figure 1 – (A) Optimized structure (LANL2DZ/6-31G*) for the Pd₂-Spm isolated molecule, and corresponding atom numbering. (B) X-ray structure for Pd₂-Spm. (Preferred conformation in the solid state with the inversion center highlighted by the blue dashed line). (C) Crystal structure arrangement for Pd₂-Spm.

This complex was shown to display interesting antiproliferative properties against cancer cells,^{15,16} although it presents a quite different chemical composition and structure from the array of active Pd(II) compounds reported in the literature to date. The understanding of the SAR's ruling this type of compound's activity is fundamental for interpreting the biochemical mechanisms underlying their biological effect (*e.g.* cytotoxic), thus allowing a rational design of new Pd-based anticancer drugs.

Vibrational spectroscopy has proven to be one of the most powerful techniques for performing conformational studies in biologically relevant molecules (including inorganic compounds). Inelastic neutron scattering (INS) spectroscopy is particularly well suited to study materials containing hydrogen atoms, since the scattering cross section for hydrogen (^1H) (about 80 barns) is much larger than for most other elements (at most *ca.* 5 barns). The neutron scattering cross-section of an element is a characteristic of each isotope and independent of the chemical environment. During the scattering event, a fraction of the incoming neutron energy can be used to cause vibrational excitation, and the vibrational modes with the largest hydrogen displacements will dominate the spectrum. Therefore, INS can be especially important in solids in which the molecular units are linked together by hydrogen close contacts, with the lowest-frequency vibrations expected to be most affected. Combining experimental vibrational spectroscopy results with quantum mechanical calculated data allows a deeper understanding of the correlation between the system's molecular properties (structure and conformation) and the corresponding spectra.

In this study, quantum mechanical calculations were carried out for $\text{Pd}_2\text{-Spm}$ at the DFT level, since this approach has shown to deliver accurate results for this type of systems.¹⁷⁻¹⁹ A theoretical model previously reported by the authors for a mononuclear Pd(II) compound bearing non-chelating ligands¹⁷ was presently evaluated as to its suitability for the highly flexible polynuclear polydentate chelate $\text{Pd}_2\text{-Spm}$. The accuracy of the calculated results was assessed by comparison with the experimental data available on this chelate – both reported X-ray structural information¹⁴ and the vibrational results gathered in this work.

2. EXPERIMENTAL

2.1 Synthesis of Pd₂-Spm

Potassium tetrachloropalladate(II) (K₂PdCl₄, 98%) and spermine (≥97%) were acquired from Sigma (Sintra, Portugal) and used without further purification.

The synthesis of Pd₂-Spm was carried out following an optimized procedure based on the published synthetic route.¹⁴ Briefly, 2 mmol of K₂PdCl₄ were dissolved in a minimal amount of water, and an aqueous solution containing 1 mmol of spermine was added drop wise under continuous stirring, for about 24 h. Solid (PdCl₂)₂(Spm) was formed, which was filtered and washed with pure acetone. Upon drying in an oven at 40°C overnight yellow crystals were obtained.

Yield: 68%. Elemental analysis was carried out at the Atlantic Microlab, Inc., Georgia, USA. Calculated - C: 21.56%; H: 4.70%; N: 10.06%, Cl: 25.46% and Found: C: 21.22%; H: 4.68%; N: 9.60%, Cl: 25.88%.

2.2 Vibrational Spectroscopy

Room-temperature Fourier transform Raman (FT-Raman) spectra were acquired on an RFS-100 Bruker Fourier transform Raman spectrometer, with near-infrared excitation provided by the 1064 nm line of a Nd:YAG laser. A laser power of 150 mW at the sample position was used. Each spectrum was the average of three repeated measurements of 150 scans, at 2 cm⁻¹ resolution.

The Fourier transform infrared (FTIR) spectra at room-temperature were recorded over the 400-4000 cm⁻¹ region, on a Mattson 7000 FTIR spectrometer, using a global source, a deuterated triglycine sulfate (DTGS) detector and potassium bromide pellets.

Each spectrum was composed of 32 scans, with 2 cm^{-1} resolution and triangular apodization.

The INS spectrum of the complex was obtained at the ISIS Pulsed Neutron Source of the STFC Rutherford Appleton Laboratory (United Kingdom), using the TOSCA spectrometer, an indirect geometry time-of-flight, high resolution (*ca.* 1.25% of the energy transfer), broad range spectrometer.²⁰ A crystalline sample of the complex (2-3 g) was wrapped in a 4×4 cm aluminium foil sachet, which filled the beam, and placed in a thin walled aluminium can. To reduce the impact of the Debye-Waller factor on the observed spectral intensity, the sample was cooled to *ca.* 15 K. Data was recorded in the energy range -24 to 4000 cm^{-1} and converted to the conventional scattering law, $S(Q, \nu)$ vs energy transfer (in cm^{-1}) through standard programs.

2.3 Computational Details

All calculations were performed using the Gaussian 03W (G03W) package.²¹ Both isolated molecule and two-molecule geometry were fully optimized by the Berny algorithm, using redundant internal coordinates. While the initial conformational study was carried out without symmetry constraints, once the best conformer was selected subsequent calculations were subject to symmetry constraints (C_i symmetry group). In all cases, vibrational frequency calculations were performed, at the same level of theory, to verify that the geometries corresponded to a real minimum in the potential energy surface (no negative eigenvalues) and to simulate the vibrational spectra.

Two approaches were used to describe the palladium atom: by relativistic pseudopotentials developed by Hay and Wadt,²² in a double-zeta splitting scheme, as

implemented in G03W (keyword *LANL2DZ*); or by an all-electron (AE) contracted Gaussian basis set developed by Friedlander.²³ Inclusion of a polarization function at the Pd atom, by augmenting the valence shell with an f-function ($\zeta_{\text{Pd}}=1.472$), was also tested in combination with LANL2DZ.²⁴ For the non-metal atoms, several AE basis were tested: 6-31G*, 6-31G**, 6-31+G(2d) and 6-31+G(2df) (as defined in G03W), either alone or simultaneously in distinct combinations schemes for different atoms (mix 1 and mix 2), as described in Table 1. Natural Bond Orbital (NBO) analysis was also performed. The basis sets were tested at the DFT theory level, using the mPW1PW method which comprises a modified version of the exchange term of Perdew-Wang and the Perdew-Wang 91 correlation functional,^{25,26} which has been shown to be advantageous over other DFT functionals for both linear amine ligands and their Pt(II)/Pd(II) complexes.^{17,18,27} The B97D DFT, which includes semi-empirical corrections for dispersion, was also tested.²⁸ In order to account for the basis set superposition error (BSSE) in the two-molecule model calculation, geometries were optimized within the scheme of Boys-Bernardi²⁹ (as implemented in G03W, by use of the keyword counterpoise). The SCRF (self-consistent reaction field) calculations were performed considering the aqueous solution ($\epsilon=78.39$) using default parameters for the UAHF (United Atom Topological Model) radii model.²¹

3. Results and Discussion

3.1 Conformational analysis

The reported X-ray structure for the Pd₂-Spm molecule¹⁴ (Figure 1) comprises both Pd(dap)Cl₂ units (dap=1,3-diaminopropane, H₂N(CH₂)₃NH₂) in a relative *trans* arrangement. The chelate ring assumes a chair conformation, while the central putrescine-like moiety has an all-*trans* geometry. Careful inspection of this crystalline

lattice structure (Figure 1.C) suggests the formation of intermolecular H-bonds between the Pd(dap)Cl₂ fractions of adjacent molecules, namely Cl₁;Cl₂⋯H₁,H₂(N₁) and Cl₂⋯H₉(N₂), as well as a Cl₁⋯H₁₀(C₄) interaction. The more hydrophobic methylene groups, in turn, should not be involved in this type of close contacts.

Taking the determined x-ray geometry as the starting point, a rotational conformational analysis was performed for the Pd₂-Spm isolated molecule (Figure S1 of the supplementary material), in the light of a previous work on the cDDPd mononuclear complex.¹⁷ We were interested in testing the relative stability of different *cis/trans* conformations (regarding the two metal centres relative to each other), all-*trans* and non-*trans* configuration of the amine linker and the presence or absence of co-planarity of the metal central relative to the central amine linker. The minimum energy conformer obtained for Pd₂-Spm differs significantly from the reported X-ray structure. As the present work aims at a study to understand the properties of a molecule in the solid state, this type of single molecule conformational studies may not be adequate to accurately represent these large polynuclear systems, since the intermolecular interactions between neighbouring molecules in the crystal lattice (Figure 1.C) impact their structure to a much larger extent than for mononuclear complexes playing a non-negligible role on the maintenance of the overall chelate's conformation. The number of rotational conformers turns this type of study prohibitive for a system such as this one as it is too large and presents too many degrees of freedom.

In fact, taking the isomer that we knew that was the one present in the solid state, we screened it with the license free program Avogadro³⁰ (using molecular mechanics (UFF)) which predicted 242 conformers. Twenty of them, among the ones with small energy, were chosen to perform a more thorough study (Figure S1) as we were

interested mainly in testing the relative stability of cis/trans conformations (regarding the two metal centres relative to each other), all-*trans* and non-*trans* configuration of the amine linker and co-planarity regarding the metal central relative to the central amine linker.

Although plane-wave calculations have been carried out by the authors³¹⁻³⁴ to predict solid state arrangements, this type of approach is not easily accessible for this particular dinuclear chelate due to the large dimensions of the corresponding unit cell. In view of these limitations, and taking into account that the aim of this study is to predict the properties of Pd₂-Spm in the solid state, the lowest-energy conformer found for the isolated molecule (conformer 1, Figure S1) was not considered in the further analysis, but rather the optimized Pd₂-Spm isolated molecule that matches the X-ray data (Figure 1.A).

3.2 Structural analysis

The single molecule of Pd₂-Spm taken from the X-ray file which was previously optimized without symmetry constraints (conformer 5, Figures S1 and 1.A) was then reoptimized under symmetry constraints (C_i symmetry group), yielding the structural parameters comprised in Table 2. Also presented, are the differences between the experimental and calculated values (Δ -values), and the corresponding overall errors ($\Delta\Delta$ -values), calculated as previously described for cisplatin¹⁸. In general, the larger deviations from the experimental values are verified for the Pd(dap)Cl₂ moiety. It was hypothesized that these could be mainly due to: (i) poor description of the metal centre and/or (ii) neglecting the intermolecular interactions present in the crystal lattice.

Considering hypothesis (i), the LANL2DZ ECP was augmented with an f-polarization function at the Pd centre, and the all-electron basis set of Friedlander²³ was

tested in the metal ion. While augmenting the Pd valence shell did not lead to a significant change (results not shown), the use of an AE basis at the Pd ion caused clear changes in the complex's structural parameters. From analysis of Table 2, it is evident that the use of an AE basis set on Pd(II) greatly improves the prediction of the Pd-N bond length, which had been previously overestimated by all theoretical approaches. However, this leads to a worsening of the Pd-Cl bond length values (as well as of some bond angles involving chlorine), in the order: for the Pd-Cl bond, LANL2DZ/6-31G* > AE/mix1 > AE/6-31G*~AE/mix2 > AE/6-31G+(2d) > AE/6-31G**;

for the Cl-Pd-Cl angle, LANL2DZ/6-31G* > AE/6-31G** > AE/mix2 > AE/mix1~AE/6-31G* > AE/6-31G+(2d); for the Cl-Pd-N angle, LANL2DZ/6-31G* > AE/6-31G** > AE/mix2 > AE/mix1~6-31G* > AE/6-31G+(2d). Interestingly, the addition of a polarization function to the hydrogen atom (AE/6-31G* → AE/6-31G**) leads to a better overall agreement relative to the experimental values of the Cl-Pd-Cl and N-Pd-Cl angles, which can probably be due to a better description of the neighbouring molecular groups bearing hydrogens. However, including higher polarization functions on the non-hydrogen atoms (AE/6-31+G(2d)) did not lead to an enhancement of the overall $\Delta\Delta$ values. Coupling the AE basis set tested for Pd(II) with a combination of different AE basis sets for the remaining atoms (mix1 or mix2) yielded better $\Delta\Delta$ values but did not solve the problem entirely. While mix1, which involves more extensive basis sets for the chlorine and nitrogen atoms (Table 1), led to a significant improvement of the Pd-Cl bond length, it did not produce more accurate values for the bond angles. In turn, while mix2, which extends the improvement of the basis set to the carbon, chlorine and nitrogen atoms (Table 1), yields better Δ values for the angles, it worsens some of the bond lengths.

Regarding hypothesis (ii), calculations for a two-molecule species (Figure S2, supplementary material) based on the X-ray structure reported for the complex, were performed to verify if accounting for intermolecular interactions could improve the results. Considering this model led to an improvement of the calculated Pd-N bond length, at the cost of a worsening of the values for the Pd-Cl bond (Table S1, supplementary material). However, although the bond angles involving the metal centre were greatly improved, the overall error was not much lower than that obtained for the isolated molecule. The reason for this probably lies on the fact that only two Pd₂-Spm molecules are not enough to represent all the intermolecular interactions occurring in the solid lattice, where one Pd₂-Spm entity is surrounded by six neighbouring molecules (Figure 1.C). Accounting for a six-molecule model using the present theoretical approach is, however, not feasible. A calculation for the two-molecule structure was also performed with the new B97D DFT, which accounts for dispersion corrections allowing a better description of the intermolecular interactions, but without significant improvement in the results (not shown). Although the structural experimental parameters are given for the solid state, SCRF results were also performed as an assessment for intermolecular interactions, not between similar molecules, but with other molecules such as the ones occurring when simulating an aqueous solution. The results gathered in Table 2 show that, interestingly, SCRF results are the ones that present the lowest bond lengths deviations obtained for the linking amine fragment N₁-C₁-C₂-C₃-N₂ and N₂-C₄. It also presents the lowest deviation values for the Cl₁-Pd-Cl₂, N₁-Pd-N₂ and Cl₁-Pd-N₁ angles, the ones more prone to establish intermolecular interactions. The reason for an improvement of these results when compared to the two-molecule structures, even when comparing different physical states, may be the

limitation of considering only a two-molecule system instead of a higher one with at least two layers of molecules, below and above. These results shed some light and hope on a very accurate prediction when plane-wave tools become available for the study of these compounds.

The theoretical estimate of the chelate's structural parameters is of the utmost importance for the prediction of reliable SAR's for the complex. When comparing the experimental bond lengths for different compounds of the same type, it is interesting to verify that within Pd₂-Spm, the Pd-N bonds (203.2 pm average value, Table 2) are shorter relative to the parent mononuclear compound cDDPd (206.0 pm)³⁵, while the Pd-Cl ones are longer (231.5 pm vs. 227.5 pm).³⁵ Natural Bond Orbital (NBO) calculations through the calculated Wiberg bond indexes - an indicator that reflects the strength of the bond - also predict this trend which is interestingly correlated with the biological activity of the complexes involved (Figure 2). In fact, regarding the human breast cell line MDA-MB-231 cell line, the IC₅₀ obtained at 24h are for cDDPd ≥ 100μM, for Pd(dap)Cl₂ > 100 μM and for Pd₂-Spm = 4.7μM.

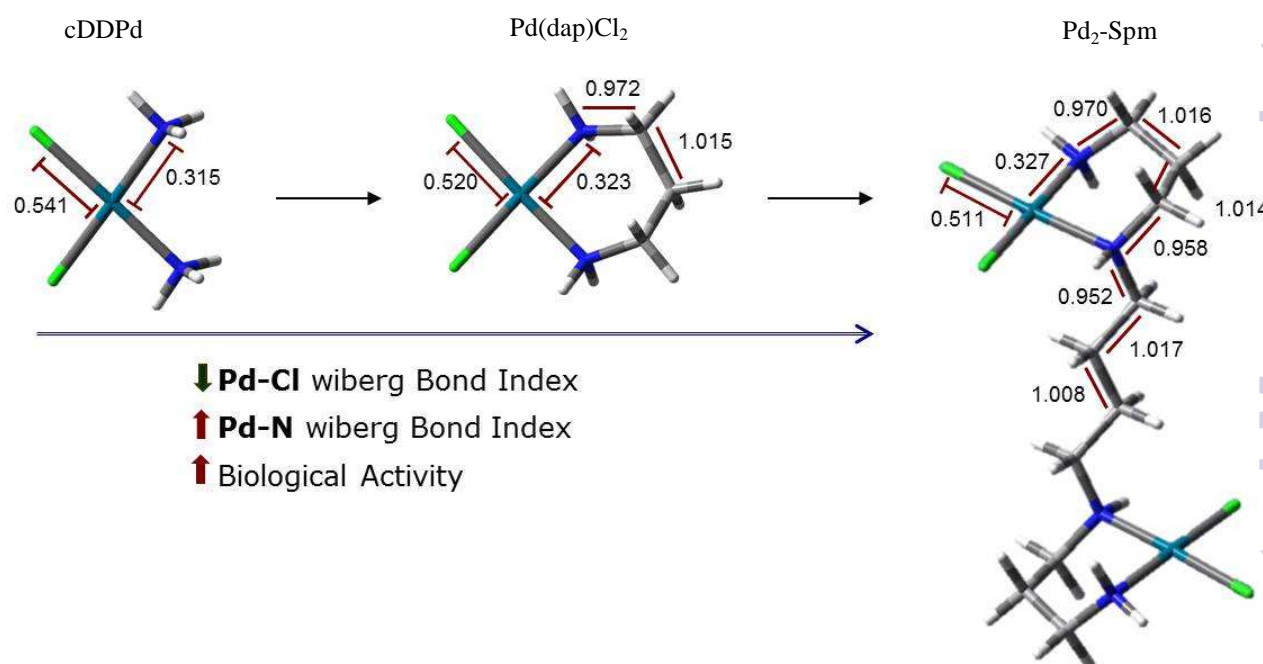
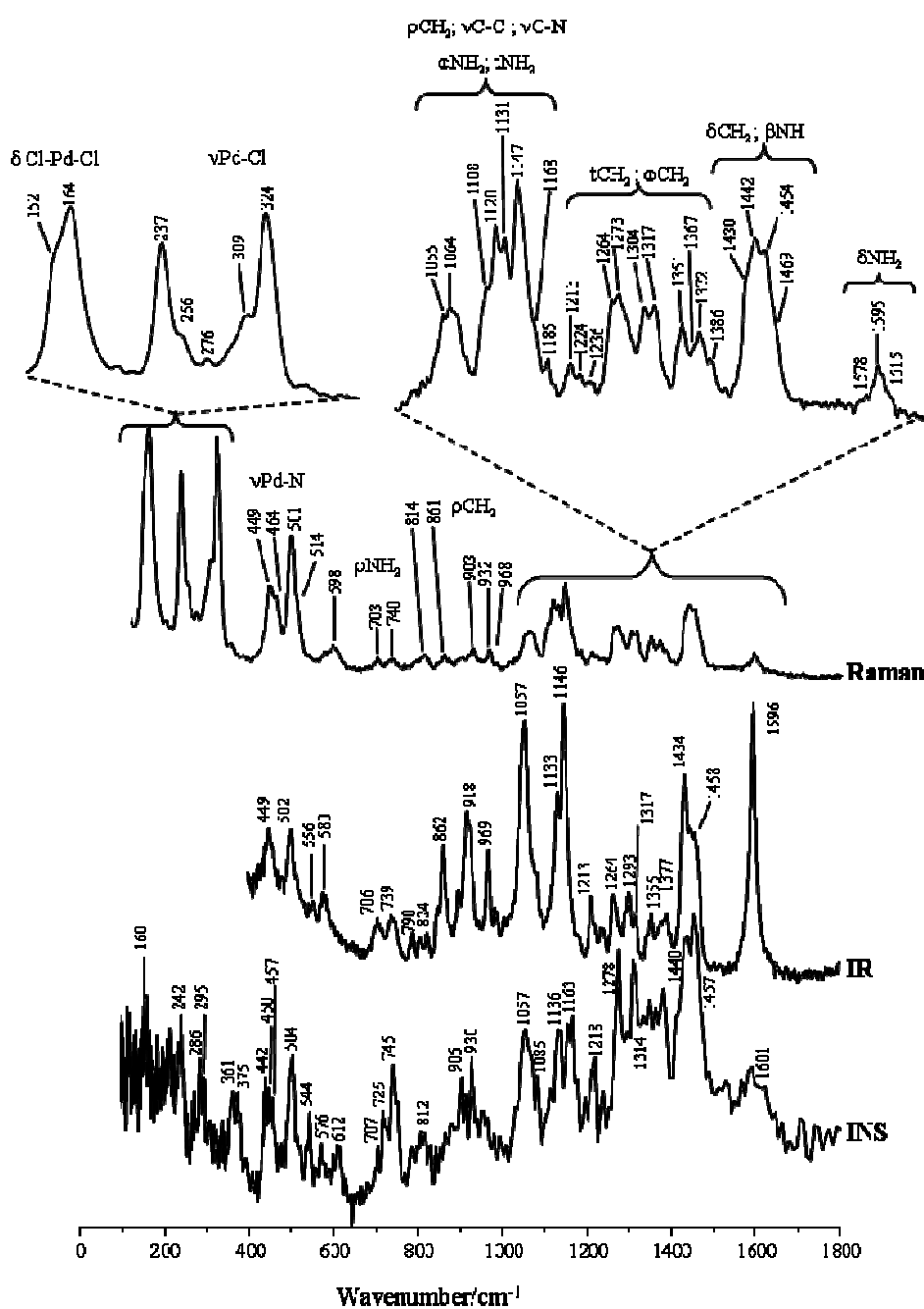


Figure 2 - Variation of Wiberg bond indexes (WBI) for three different Pd(II) complexes: cDDPd (cis-diamminodichloropalladium(II)), Pd(dap)Cl₂ (1,3-diamminopropane-dichloropalladium(II)) and Pd₂-Spm ($\{\mu\text{-}\{N,N'\text{-bis}[(3\text{-amino-}\kappa N)\text{propyl}]butane\text{-}1,4\text{-diamine-}\kappa N:\kappa N'\}\}$ tetrachloro-dipalladium (II)). (White – H; Grey – C; Blue – N; Green – Cl; Cyan – Pd(II)). IC₅₀ values for the MDA-MB-231 cell line at 24h are $\geq 100\mu\text{M} > 100\mu\text{M}$ and $4.7\mu\text{M}$, respectively.

The mode of action of this type of metal-based compounds is recognized to be through interaction, *via* covalent binding, to DNA.^{36,37} Although the exact mechanism for Pd(II) complexes is not as well established as for their Pt(II) analogues, they are expected to have a rather similar behaviour due to their similar chemical characteristics. The anticancer properties of the well-known chemotherapeutic drug cisplatin relies on the binding of Pt(II) to the nitrogen (N⁷) of the DNA bases.³⁶⁻³⁸ This step must be preceded by an intracellular drug activation process through aquation, that involves the hydrolysis of the chlorine ligands. Accordingly, it is expected that the DNA binding ability of these amine-based Pd(II) complexes increases with weakening of the Pd-Cl bonds, as evidenced in Figure 2. Although more systems are needed for an unequivocal and trustful correlation, these results prompt the investigation of this possible correlation and stress the importance of this type of study, even in the solid state.

3.3 Vibrational analysis

$\text{Pd}_2\text{-Spm}$ has 132 vibrational modes, 66 of A_u symmetry (infrared active) and 66 bearing A_g symmetry (Raman active). All the modes are INS active, since there are no selection rules for this non-optical vibrational spectroscopy technique (Figure 3).



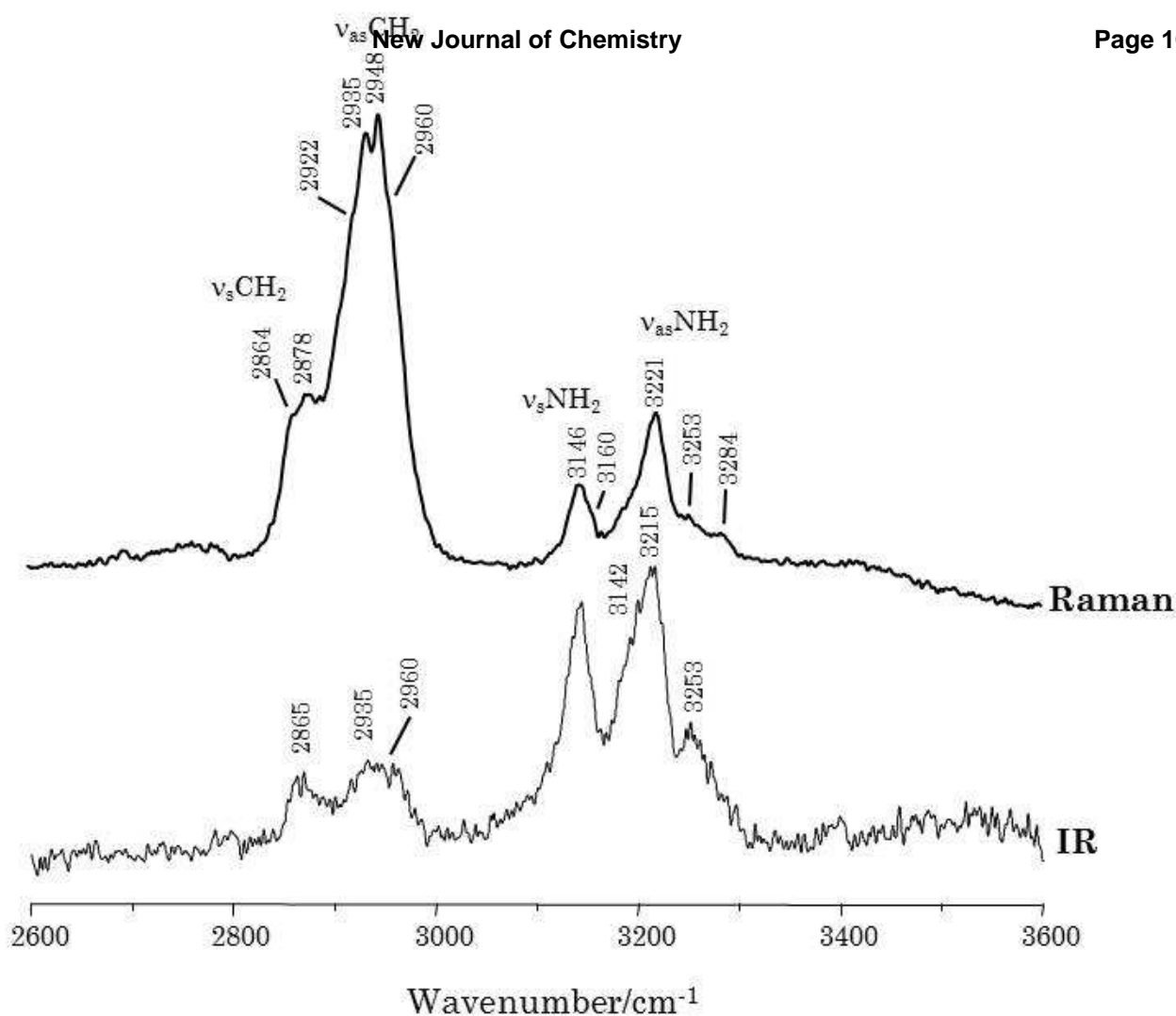


Figure 3 – Experimental vibrational spectra (Raman, IR and INS) for Pd₂-Spm.

The assignment of the vibrational spectra of Pd₂-Spm, as well as the calculated wavenumbers at the LANL2DZ/6-31G* theory level are presented in Table 3. It has been shown previously that the small enhancement obtained with higher theory levels is not worth the associated computational cost.^{17,18} Some vibrational modes (as well as the corresponding nomenclature used throughout the text) are schematically represented in Figure 4.

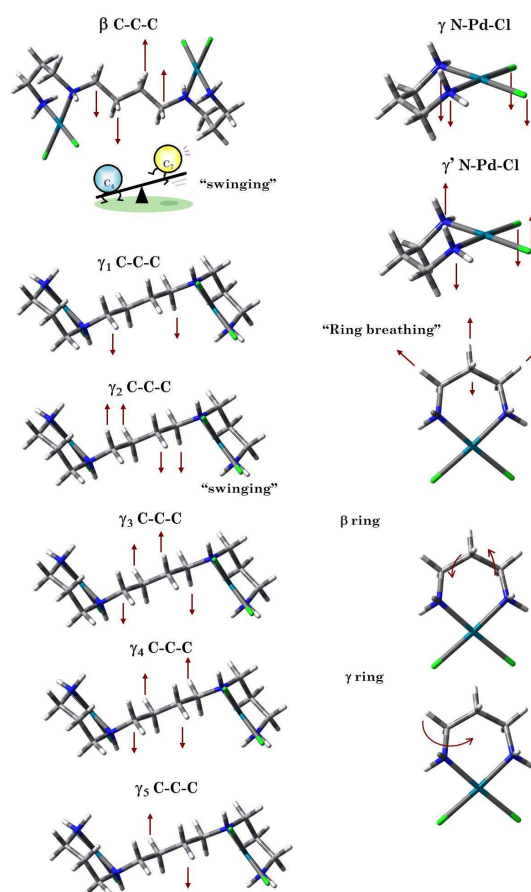


Figure 4 – Schematic representation of selected vibrational modes for Pd₂-Spm (and nomenclature used along this work).

As the metal units are linked by the aliphatic amine spermine, some low frequency vibrations are similar to the reported LAM and TAM modes previously assigned for this polyamine.^{40,41} However, they were given alternative designations in this work since Pd-coordinated Spm does not constitute a free “linear bead system” as illustrated in Figure 4.

The inspection of Figure 3 allows to determine the importance and complementarity of the different techniques used. Raman spectroscopy features more intense CH₂ stretching bands and also presents more prominent bands regarding the metal atoms. Also, the different bands regarding the organic moiety of the molecule are not quite well resolved appearing broad and overlapped. Nonetheless, the resolution of

the band relative to the metal centre using Raman technique allows to distinguish the different vibrational frequencies, particularly for the Pd-N bond. As the environment of Pd-N₁ is different from Pd-N₂, these modes are not degenerated and it is possible to identify 4 bands for the ν Pd-N vibration instead of 2 bands if their environment was the same, i.e., having a symmetrical centre. This feature is not as clear when using the other vibrational techniques. IR and INS bands in turn appear much more defined in the region ranging from 400-1800 cm⁻¹ allowing the detection of a higher number of vibrational modes. Particularly important and characteristic of the IR technique is the very intense and well defined deformation band of NH₂ at 1596 cm⁻¹. When analysing the crystal structure packing unit, only one intermolecular hydrogen bond is available to the NH₂ group (N₁)H₂-Cl₂ (248.2 angstrom), the next shortest contact for NH₂ is a weak intramolecular interaction (N₁)H₁-Cl₁ (268.7 angstrom). This quite defined δ NH₂ band, supports this occurrence as it is not as broad as the one expected for a group highly involved in strong hydrogen networking. The INS technique in turn perfectly resolves the lower rocking modes of the CH₂ and NH₂ oscillators (which are almost imperceptible by Raman), as well as the ring structure torsions bands (almost absent from the IR and Raman spectra). These features stress the importance of using these three complementary vibrational techniques, especially for this type of complexes which tend to form intramolecular ring structures.

The vibrational modes from the spermine ligand were reasonably predicted by the calculations, despite some deviations due to anharmonicity and/or intermolecular interactions. The major differences were verified for the modes involving the atoms directly bound to the metal atom, which cannot be justified in terms of anharmonicity since there is not a uniform pattern in the prediction of the wavenumbers. In order to

determine whether this was a particular effect of this chelate, calculations were performed, at the same theory level (LANL2DZ/6-31G*), for a few other Pd(II) complexes with different amine ligands. The data thus gathered is collected in Table 4 as the scaling factor needed to match the calculated wavenumbers to the experimental ones. In every case, the theoretically predicted Pd-N stretching mode was found to be underestimated, while $\nu(\text{Pd-Cl})$ and $\nu(\text{NH}_3/\text{NH}_2)$ were overestimated. Hence, this lack of accordance is independent of the type of complex investigated, the main issue probably remaining to be the description of the modes involving the metal centre.

Additionally, neither the AE approach to describe the metal centre nor the two-molecule model calculations led to a noticeable improvement of the corresponding vibrational modes. In fact, it was previously verified by the authors¹⁷ that an enhancement in the calculated structural parameters is not always accompanied by a corresponding improvement of the accuracy of the vibrational frequencies.

Although a straightforward comparison with the SCRF results (Table 3) cannot be performed, some comments are in order. Actually, the vibrations relative to the stretching modes of NH_2 and CH_2 groups are greatly improved and comparable to the experimental values. Also, the symmetric stretching mode Pd-N is also improved, but not the antisymmetric one. A better agreement with the experimental value is also obtained for the C-N-C torsion of the ring structure. However, many other vibrational modes are poorly predicted, such as the NH_2 and CH_2 scissoring and most wagging, twisting and rocking modes of the CH_2 groups. Moreover, many stretching vibrational modes for the C-C and C-N bonds fail to be predicted, as well as the $\nu(\text{Pd-Cl})$ ones. Nonetheless, the improvement obtained for the groups expected to be strongly involved

in intermolecular interactions should be of reference for future studies on this type of systems.

4. CONCLUSIONS

In the present work, a complete vibrational study of a dinuclear Pd(II) complex displaying a promising antiproliferative activity was undertaken, by a combined spectroscopic and quantum mechanical calculations methodology. FTIR, Raman and INS spectra were recorded and the theoretical analysis was carried out at the DFT level, for both the isolated molecule and a two-molecule model.

It was shown that the intermolecular interactions within the crystal lattice are of the utmost importance for this type of polynuclear polyamine chelates. A simple isolated molecule calculation was found not to suffice for predicting the molecular properties of such a system, as opposed to what has been reported (by the authors) for their mononuclear counterparts. Although the calculations performed for the two-molecule species yielded slightly better results, the structural improvements were not noteworthy. Furthermore, whenever there are no X-ray data available and several possible two-molecule geometries to be tested, this type of approach becomes excessively demanding (in terms of computational costs).

In order to further improve the representation of this kind of Pd(II)-amine complexes, it is of paramount importance to develop new basis sets as was recently carried out for Pt(II) complexes^{19,41} (which was out of the scope of this work). At the moment, it seems that the precise estimate of one type of metal-ligand bond length leads to the unbalance of the other one, and an improvement of the bond lengths implies a worse description of the bond angles. Therefore, when considering only the prediction

of the structural parameters, some doubts can arise as to the most suitable theoretical approach. For the representation of the vibrational profiles, in turn, the LANL2DZ/6-31G* theory level was shown to attain a high degree of accordance with the experiment, while the enhancement obtained with higher theory levels was not worth the associated computational cost. Optimization of the theoretical methodology for this kind of polynuclear polyamine Pd(II) agents will hopefully allow the establishment of accurate and reliable SAR's and to predict other important properties relevant for their anticancer capacity. Finally, while plane-wave calculations are of utmost importance for estimating the properties of a molecule in the solid state, an up-to-date all-electron basis set for palladium(II) is also crucial, since studies for an isolated molecule cannot be ruled out for large polynuclear complexes bearing biological properties.

The data obtained in this work shows an inverse relationship between the strength of the Pd-Cl bond and the antiproliferative effect of Pd₂-Spm against cancer cells, i.e., the weaker the Pd-Cl bonds the higher the complex's activity. The antiproliferative activity of such a compound is determined by several other factors. However, this evidence may indicate that these Pd(II)-amine chelates (comprising cisplatin-like moieties) could display a similar mode of action to that of cisplatin, involving chloride hydrolysis inside the cell as their major activation step.

Acknowledgements

The authors acknowledge financial support from the Portuguese Foundation for Science and Technology – UID/MULTI/00070/2013. SF thanks FCT - the Portuguese Foundation for Science and Technology – SFRH/BPD/75334/2010 scholarship. The INS work was supported by the European Commission under the 7th Framework Programme through the Key Action: Strengthening the European Research Area, Research Infrastructures (Contract n^o: CP-CSA_INFRA-2008-1.1.1 Number 226507-NMI3). Laboratório Associado CICECO (University of Aveiro, Portugal) is also acknowledged for access to the FT-Raman and FTIR spectrometers.

References

- 1 S. Ray, R. Mohan, J. K. Singh, M. K. Samantaray, M. M. Shaikh, D. Panda, and P. Ghosh, *J. Am. Chem. Soc.* 2007, **129**, 15042-15053.
- 2 E. Gao, C. Liu, M. Zhu, H. Lin, Q. Wu and L. Liu., *Anti-cancer Agents Med. Chem.* 2009, **9**, 356-368.
- 3 F. Aria, B. Cevatemrea, E. I. I. Armutakb, N. Aztopala, V.T. Yilmazc and E. Ulukaya, *Bioorg. Med. Chem.* 2014, **22**, 4948-4954.
- 4 A. Garoufis, S. K. Hadjikakou and N. Hadjiliadis, *Coord. Chem. Rev.* 2009, **253**, 1384-1397.
- 5 E. Sindhuja, R. Ramesh, N. Dharmaraj and Y. Liu, *Inorg Chim Acta* 2014, **416**, 1-12.
- 6 J. L. Butour, S. Wimmer, F. Wimmer and P. Castan, *Chem.-Biol. Interact.* 1997, **104**, 165-178.
- 7 F. Shaheen, A. Badshah, M. Gielen, C. Gieck, M. Jamil and D. Vos, *J. Organomet. Chem.* 2008, **693**, 1117-1126.
- 8 F. Shaheen, A. Badshah, M. Gielen, G. Croce, U. Florke, D. de Vos and S. Ali, *J. Organomet. Chem.* 2010, **695**, 315-322.
- 9 H. A. El-Asmy, I. S. Butler, Z. S. Mouhri, B. J. Jean-Claude, M. S. Emmam and S. I. Mostafa, *J. Mol. Struct.* 2014, **1059**, 193-201.
- 10 P. Vranec and I. Potocnak, *J. Mol. Struct.* 2013, **1041**, 219-226.
- 11 R. A. Haque, A. W. Salman, S. Budagumpi, A. A. A. Abdullah and A. M. S. A. Majid, *Metallomics* 2013, **5**, 760-769.
- 12 M. P. M. Marques, *ISRN Spectrosc.* 2013, **2013**, 1-29.
- 13 D. Kovala-Demertzi, A. Alexandratos, A. Papageorgiou, P. N. Yadav, P. Dalezis and M. A. Demertzis, *Polyhedron* 2008, **27**, 2731-2738.
- 14 G. Codina, A. Caubet, C. López, V. Moreno and E. Molins, *Helv. Chim. Acta* 1999, **82**, 1025.
- 15 A. S. Soares, S. M. Fiuza, M. J. Gonçalves, L. A. E. Batista de Carvalho, M. P. M. Marques and A. M. Urbano, *Lett. Drug Des. Disc.* 2007, **4**, 460-463.
- 16 S. M. Fiuza, J. Holy, L. A. E. Batista de Carvalho and M. P. M. Marques, *Chem. Biol. Drug Des.* 2011, **77**, 477-488.
- 17 S. M. Fiuza, A. M. Amado, H. F. Dos Santos, M. P. M. Marques and L. A. E. Batista de Carvalho, *Phys. Chem. Chem. Phys.* 2010, **12**, 14309-14321.
- 18 A. M. Amado, S. M. Fiuza, M. P. M. Marques and L. A. E. Batista de Carvalho, *J. Chem. Phys.* 2007, **127**, 185104.
- 19 D. Paschoal, B. L. Marcial, J. F. Lopes, W. B. De Almeida and H. F. Dos Santos, *J. Comp. Chem.* 2012, **33**, 2292-2302.
- 20 <http://www.isis.stfc.ac.uk/>
- 21 M. J. Frisch, G. W. Trucks, H. B. Schlegel, G. E. Scuseria, M. A. Robb, J. R. Cheeseman, J. A. Montgomery Jr., T. Vreven, K. N. Kudin, J. C. Burant, J. M. Millam, S. S. Iyengar, J. Tomasi, V. Barone, B. Mennucci, M. Cossi, G. Scalmani, N. Rega, G. A. Petersson, H. Nakatsuji, M. Hada, M. Ehara, K. Toyota, R. Fukuda, J. Hasegawa, M. Ishida, T. Nakajima, Y. Honda, O. Kitao, H. Nakai, M. Klene, X. Li, J. E. Knox, H. P. Hratchian, J. B. Cross, V. Bakken, C. Adamo, J. Jaramillo, R. Gomperts, R. E. Stratmann, O. Yazyev, A. J. Austin, R. Cammi, C. Pomelli, J. W. Ochterski, P. Y. Ayala, K. Morokuma, G. A. Voth, P. Salvador, J. J. Dannenberg, V. G. Zakrzewski, S. Dapprich, A. D. Daniels, M. C. Strain, O.

- Farkas, D. K. Malick, A. D. Rabuck, K. Raghavachari, J. B. Foresman, J. V. Ortiz, Q. Cui, A. G. Baboul, S. Clifford, J. Cioslowski, B. B. Stefanov, G. Liu, A. Liashenko, P. Piskorz, I. Komaromi, R. L. Martin, D. J. Fox, T. Keith, M. A. Al-Laham, C. Y. Peng, A. Nanayakkara M. Challacombe, P. M. W. Gill, B. Johnson, W. Chen, M. W. Wong, C. Gonzalez and J. A. Pople, Gaussian 03, Revision D.01, Gaussian, Inc., Wallingford, CT, 2004.
- 22 P. J. Hay and W. R. Wadt, *J. Chem. Phys.* 1985, **82**, 299-310.
- 23 M. E. Friedlander, J. M. Howell and G. Snyder, *J. Chem. Phys.* 1982, **77**, 1921-1929.
- 24 A. W. Ehlers, M. Bohme, S. Dapprich, A. Gobbi, A. Hollwarth, V. Jonas, K. F. Kohler, R. Stegmann, A. Veldkamp and G. Frenking, *Chem. Phys. Lett.* 1993, **208**, 111-114.
- 25 C. Adamo and V. Barone *J. Chem. Phys.* 1998, **108**, 664-675.
- 26 J. P. Perdew, K. Burke and Y. Wang, *Phys. Rev. B* 1996, **54**, 16533.
- 27 S. Padrão, S. M. Fiuza, A. M. Amado, A. M. A. da Costa and L. A. E. Batista de Carvalho, *J. Phys. Org. Chem.* 2011, **24**, 110-121.
- 28 S. Grimme, *J. Comp. Chem.* 2006, **27**, 1787-1799.
- 29 S. F. Boys and F. Bernardi, *Mol. Phys.* 1970, **19**, 558-566.
- 30 M. D. Hanwell, D. E Curtis, D. C Lonie, T. Vandermeersch, E. Zurek and G. R. Hutchison; *J. Cheminform.* 2012, **4**, 17.
- 31 R. L. Lopes, M. P. M. Marques, R. Valero, J. Tomkinson and L. A. E. Batista de Carvalho, *Spectrosc. Int. J.* 2012, **27**, 273-292.
- 32 M. P. M. Marques, R. Valero, S. F. Parker, J. Tomkinson and L. A. E. Batista de Carvalho, *J. Phys. Chem. B* 2013, **117**, 6421- 6429.
- 33 R. L. Lopes, R. Valero, J. Tomkinson, M. P. M. Marques and L. A. E. Batista de Carvalho, *New J. Chem* 2013, **37**, 2691–2699.
- 34 M. P. M. Marques, L. A. E. Batista de Carvalho, R. Valero, N. F. L. Machado and S. F. Parker, *Phys. Chem. Chem. Phys.* 2014, **16**, 7491-7500.
- 35 S. D. Kirik, L. A. Solovyov and M. L. Blokhina, *Acta Cryst.* 1996, **B52**, 909-916.
- 36 P. Banerjee, *Coord. Chem. Rev.* 1999, **190-192**, 19-28.
- 37 A. Eastman, *Biochem.* 1983, **22**, 3927-3933.
- 38 M. Kartalou and J. M. Essigmann, *Mut. Res.* 2001, **478**, 1-21.
- 39 J. P. Merrick, D. Moran and L. Radom, *J. Phys. Chem. A*, 2007, **111**, 11683–11700.
- 40 M. P. M. Marques, L. A. E. Batista de Carvalho and J. Tomkinson, *J Phys. Chem. A* 2002, **106**, 2473-2482.
- 41 L. A. E. Batista de Carvalho, M. P. M. Marques and J. Tomkinson, *J Phys. Chem. A* 2006, **110**, 12947-12954.
- 42 R. C. De Berrêdo and F. E. Jorge, *J. Mol. Struct. THEOCHEM* 2010, **961**, 107-112.

TABLE 1 - Theoretical levels considered in this study, using the mPW1PW functional.

System	Basis Set		
	Pd(II) ^a	Non-heavy atoms ^b	
Two-molecule model	LANL2DZ	6-31G*	
Isolated molecule	AE	6-31G*	
	AE	6-31G**	
	AE	6-31+G(2df)	
	AE	6-31G** (H) 6-31G* (C) 6-31+G(2d) (N) 6-31+G(2df) (Cl)	mix1
	AE	6-31G** (H) 6-31+G(2d) (C,N) 6-31+G(2df) (Cl)	mix2

^a AE stands for the all electron basis set of Friedlander²³ used at the Pd(II) ion.

^b Basis sets used generally or specifically on each atom as specified in mix1 and mix2.

TABLE 2: Experimental and calculated (mPW1PW) structural parameters for Pd₂-Spm, at different theoretical levels.

Structural Parameter	Exp ^a	Theory Level ^c													
		LANL2DZ/ 6-31G*	Δ^b	AE/ 6-31G*	Δ^b	AE/ 6-31G**	Δ^b	AE/ 6-31G+(2d)	Δ^b	AE/mix1	Δ^b	AE/mix2	Δ^b	SCRF LANL2DZ/ 6-31G*	Δ^b
Bond Length/pm															
Pd-N ₁	202.2	208.4	6.2	205.3	3.1	205.3	3.1	205.0	2.8	204.7	2.5	206.1	3.9	206.4	4.2
Pd-N ₂	204.1	209.8	5.7	205.7	1.6	205.2	1.1	205.5	1.4	205.1	1.0	205.5	1.4	208.1	4.0
Pd-Cl ₁	231.6	231.7	0.1	232.8	1.2	227.9	-3.7	233.0	1.4	232.4	0.8	228.7	-2.9	235.7	4.1
Pd-Cl ₂	231.4	232.2	0.8	233.8	2.4	229.2	-2.2	233.9	2.5	233.3	1.9	230.6	-0.8	235.4	4.0
N ₁ -C ₁	148.5	147.8	-0.7	147.2	-1.3	147.1	-1.4	147.2	-1.3	147.3	-1.2	147	-1.5	147.7	-0.8
N ₂ -C ₃	148.7	147.5	-1.2	147.1	-1.6	147.3	-1.4	147.0	-1.7	147.1	-1.6	146.9	-1.8	148.4	-0.3
C ₁ -C ₂	150.6	152.4	1.8	152.5	1.9	152.4	1.8	152.5	1.9	152.5	1.9	152.3	1.7	151.8	1.2
C ₂ -C ₃	151.8	152.7	0.9	152.8	1.0	152.6	0.8	152.8	1.0	152.8	1.0	152.6	0.8	152.2	0.4
C ₄ -C ₅	152.1	152.1	0.0	152.3	0.2	152.1	0.0	152.3	0.2	152.3	0.2	152.0	-0.1	152.0	-0.1
C ₅ -C ₆	153.3	152.6	-0.7	151.5	-1.8	152.4	-0.9	151.5	-1.8	151.5	-1.8	152.0	-1.3	152.7	-0.6
N ₂ -C ₄	148.8	147.8	1.0	147.8	-1.0	147.4	-1.4	147.7	-1.1	147.8	-1.0	147.0	-1.8	148.2	-0.6
Angles/°															
Cl ₁ -Pd-Cl ₂	93.9	96.3	2.4	99.2	5.3	97.0	3.1	99.5	5.6	99.1	5.2	97.7	3.8	93.5	-0.4
N ₁ -Pd-N ₂	90.3	92.0	1.7	91.9	1.6	91.8	1.5	92.1	1.8	92	1.7	91.7	1.4	89.7	-0.6
N ₁ -Pd-Cl ₁	88.5	85.5	-3.0	84.3	-4.2	85.5	-3.0	84.0	-4.5	84.3	-4.2	85.6	-2.9	87.8	-0.7
N ₂ -Pd-Cl ₂	87.5	86.1	-1.4	84.5	-3.0	85.7	-1.8	84.2	-3.3	84.5	-3.0	85.0	-2.5	89.0	1.5
Pd-N ₁ -C ₁	114.8	113.8	-1.0	108.5	-6.3	113.2	-1.6	108.5	-6.3	108.5	-6.3	113.1	-1.7	114.3	-0.5
Pd-N ₂ -C ₃	113.9	111.8	-2.1	112.4	-1.5	111.9	-2.0	112.4	-1.5	112.4	-1.5	112.5	-1.4	111.6	-2.3
Pd-N ₂ -C ₄	113.0	115.5	2.5	112.1	-0.9	115.3	2.3	112.1	-0.9	112.1	-0.9	114.1	1.1	114.1	1.1
N ₁ -C ₁ -C ₂	110.5	112.5	2.0	112.3	1.8	112.2	1.7	112.3	1.8	112.2	1.7	112.7	2.2	112.3	1.8
N ₂ -C ₃ -C ₂	114.3	114.5	0.2	114.4	0.1	114.1	-0.2	114.3	0.0	114.3	0.0	114.2	-0.1	114.7	0.4
C ₁ -C ₂ -C ₃	115.7	115.9	0.2	116.4	0.7	115.8	0.1	116.4	0.7	116.4	0.7	116.0	0.3	114.9	-0.8
C ₃ -N ₂ -C ₄	113.0	113.7	0.7	115.1	2.1	113.9	0.9	115.2	2.2	115.0	2.0	114.2	1.2	112.9	-0.1
N ₂ -C ₄ -C ₅	112.3	112.3	0.0	109.6	-2.7	111.7	-0.6	109.6	-2.7	109.6	-2.7	112.0	-0.3	112.4	0.1
C ₄ -C ₅ -C ₆	111.3	111.2	0.1	113.0	1.7	111.5	0.2	113.1	1.8	113.0	1.7	111.3	0.0	111.2	-0.1
$\Delta\Delta$			1.5		2.0		1.5		2.1		1.9		1.5		1.3

^a Average values for identical bonds in the molecule¹⁴. ^b Δ = Calculated value-Experimental value¹⁸

TABLE 3: Experimental (INS, Raman, FTIR) and calculated (LANL2DZ/6-31G*) vibrational wavenumbers (cm⁻¹) for Pd₂-Spm (isolated molecule in gas phase and simulated aqueous solution (SCRF)).

Experimental			Calc.	Calc.(scaled) ^a	Calc. SCRF	Calc. SCRF (scaled)	Sym.	Tentative assignment ^c
INS	Raman	FTIR						
		3253	3588	3408/3337 ^b	3463	3290/3221 ^b	A _u	v _{as} NH ₂
	3221		3588	3408/3337 ^b	3462	3289/3220 ^b	A _g	v _{as} NH ₂
		3215	3484	3309/3240 ^b	3369	3200/3133 ^b	A _u	vNH
			3484	3309/3240 ^b	3367	3198/3131 ^b	A _g	vNH
		3142	3483	3309/3239 ^b	3363	3195/3128 ^b	A _u	v _s NH ₂
	3146		3483	3309/3239 ^b	3362	3194/3127 ^b	A _g	v _s NH ₂
			3165	3006	3127	2970	A _u	v _{as} CH ₂ (ring)
			3165	3006	3126	2969	A _g	v _{as} CH ₂ (ring)
			3150	2992	3132	2975	A _u	v _{as} CH ₂ (chain)
		2960	3137	2980	3120	2964	A _u	v _{as} CH ₂ (ring)
	2960		3137	2980	3120	2964	A _g	v _{as} CH ₂ (ring)
2950	2948		3130	2973	3128	2971	A _g	v _{as} CH ₂ (chain)
	2935		3126	2969	3043	2891	A _g	v _{as} CH ₂ (ring)
		2935	3126	2969	3042	2890	A _u	v _{as} CH ₂ (ring)
			3112	2956	3110	2954	A _u	v _{as} CH ₂ (chain)
	2922		3110	2954	3094	2939	A _g	v _{as} CH ₂ (chain)
			3092	2937	3063	2910	A _u	v _s CH ₂ (chain)
			3087	2932	3069	2915	A _g	v _s CH ₂ (ring)
			3087	2932	3069	2915	A _u	v _s CH ₂ (ring)
			3085	2930	3056	2903	A _g	v _s CH ₂ (ring)
			3085	2930	3056	2903	A _u	v _s CH ₂ (ring)
	2878		3083	2929	3053	2900	A _g	v _s CH ₂ (chain)
			3078	2924	2999	2849	A _u	v _s CH ₂ (ring)
			3078	2924	2995	2845	A _u	v _s CH ₂ (ring)
	2864		3051	2898	3040	2888	A _g	v _s CH ₂ (chain)
		2865	3051	2898	3038	2886	A _u	v _s CH ₂ (chain)
1601	1595		1699	1614/1580 ^b	1661	1578/1545	A _g	δNH ₂
		1596	1699	1614/1580 ^b	1660	1577/1544	A _u	δNH ₂
			1539	1462	1532	1455	A _u	δCH ₂ (chain)
	1469		1537	1460	1526	1450	A _g	δCH ₂ (chain)
1457		1458	1529	1452	1511	1435	A _u	δCH ₂ (ring)
	1454		1527	1450	1510	1434	A _g	δCH ₂ (ring)
		1449	1524	1448	1507	1431	A _u	δCH ₂ (ring)
1440	1442		1523	1447	1506	1431	A _g	δCH ₂ (ring)
			1511	1435	1509	1433	A _u	δCH ₂ (ring)
			1508	1432	1488	1413	A _g	δCH ₂ (ring)
		1434	1508	1432	1488	1413	A _u	δCH ₂ (chain)
	1430		1504	1429	1497	1422	A _g	δCH ₂ (chain)
			1486	1412	1517	1441	A _g	βNH
			1485	1411	1516	1440	A _u	βNH
1385	1386		1460	1387	1444	1372	A _g	ωCH ₂ (chain)
		1377	1455	1382	1434	1362	A _u	ωCH ₂ (chain)
	1372		1436	1364	1452	1379	A _g	ωCH ₂ (ring)
1365			1432	1360	1451	1378	A _u	ωCH ₂ (ring)
	1367		1431	1359	1428	1356	A _g	ωCH ₂ (ring)
1351		1355	1424	1353	1415	1344	A _u	ωCH ₂ (ring)
	1351		1406	1336	1400	1330	A _g	ωCH ₂ (ring)
1338			1398	1328	1399	1329	A _u	ωCH ₂ (ring)
1314		1317	1377	1308	1350	1280	A _u	tCH ₂ (chain)
	1317		1372	1303	1361	1285	A _g	tCH ₂ (ring)
1299	1304		1371	1302	1375	1293	A _g	ωCH ₂ (chain)
		1293	1368	1299	1353	1282	A _u	tCH ₂ (ring)
			1361	1293	1347	1264	A _g	tCH ₂ (chain)

1278	1273		1348	1280	1297	1216	A _g	tCH ₂ (chain)
1256		1264	1334	1267	1331	1255	A _u	tCH ₂ (ring)
1240		1238	1304	1239	1280	1187	A _u	ωCH ₂ (chain)
1218	1224		1295	1230	1321	1253	A _g	tCH ₂ (ring)
	1213		1287	1223	1319	1248	A _g	tCH ₂ (ring)
		1213	1281	1217	1314	1232	A _u	tCH ₂ (ring)
1163		1179	1261	1198	1250	1167	A _u	tNH ₂ + tCH ₂ (chain)
	1185		1244	1182	1229	1143	A _g	tNH ₂ + ρCH ₂ (chain)
		1146	1184	1125	1170	1104	A _u	tCH ₂ (chain) + tCH ₂ (ring)
	1147		1167	1109	1112	1051	A _g	vC-C
1136	1131		1166	1108	1200	1120	A _g	ρCH ₂ (chain)
		1133	1163	1105	1203	1140	A _u	ωNH ₂
	1120		1142	1085	1112	1051	A _g	vC-C
			1130	1073	1162	1099	A _u	vC-N
	1108		1127	1071	1179	1111	A _g	ωNH ₂
1085		1085	1122	1066	1157	1056	A _u	vC-N
			1107	1052	1101	1040	A _u	vC-N
1070	1064		1100	1045	1095	1031	A _g	vC-C (chain)
1057	1055		1098	1043	1085	1031	A _g	vC-N
		1057	1092	1037	1016	951	A _u	vC-N
			1082	1028	1106	1046	A _g	γNH
			1065	1012	1085	1020	A _u	γNH
			1058	1005	1074	1018	A _g	vC-C
			1052	999	1001	920	A _g	vC-N
		969	1025	974	1072	965	A _u	vC-C
		918	977	928	968	912	A _u	vC-C
930	932		970	921	960	901	A _g	ρCH ₂ (ring)
		899	945	898	949	887	A _u	ρCH ₂ (chain)
			939	892	934	885	A _u	ρCH ₂ (ring)
906	903		937	890	932	857	A _g	ρCH ₂ (ring)
	861		884	840	902	854	A _g	ρCH ₂ (ring)
		862	883	839	899	796	A _u	ρCH ₂ (ring)
812	814		826	785	838	793	A _g	ρCH ₂ (ring)
789		790	823	782	835	773	A _u	ρCH ₂ (ring)
			811	770	814	714	A _g	ρCH ₂ (chain)
			750	712	752	712	A _u	ρCH ₂ (chain)
707/725/745		706/739	680	680	750	711	A _u	ρNH ₂
	703/740		680	680	748	560	A _g	ρNH ₂
612	598		572	572	590	558	A _g	β ring
576		579	560	560	587	500	A _u	β ring
544		552	549	549	502	477	A _u	δ N-C-C (ring)
	514		531	531	526	499	A _g	δ C-N-C
			474	474	499	493	A _u	δ C-N-C
504	501	502	437	485 ^b	480	533 ^b	A _u	v _s Pd-N
			436	484 ^b	456	506 ^b	A _g	v _s Pd-N
457	464		471	471	428	428	A _g	τ CC _{ring}
450	449		398	442 ^b	499	554 ^b	A _g	v _{as} Pd-N
442		449	393	436 ^b	493	547 ^b	A _u	v _{as} Pd-N
	324	-	345	321 ^b	320	298 ^b	A _g	v _s Pd-Cl
		-	343	319 ^b	319	297 ^b	A _u	v _s Pd-Cl
361/375		-	337	337	280	280	A _u	γ ring
	309	-	326	303 ^b	300	279 ^b	A _g	v _{as} Pd-Cl
295		-	315	293 ^b	293	272 ^b	A _u	v _{as} Pd-Cl
286	276	-	282	262 ^b	242	225 ^b	A _g	δ N-Pd-N
		-	281	261 ^b	230	214 ^b	A _u	δ N-Pd-N
242	256	-	265	265	192	192	A _g	γ ring
236	237	-	249	249	310	310	A _g	β C-C-C "swinging"
216		-	222	222	349	349	A _u	"ring breathing"

		-	198	198	214	214	A _u	γ_1 C-C-C _{chain}
196	203	-	185	205 ^b	140	155 ^b	A _g	δ N-Pd-Cl
		-	179	199 ^b	136	151 ^b	A _u	δ N-Pd-Cl
168	164	-	167	167	223	223	A _g	τ C-N _{ring}
153	152	-	150	150	158	158	A _g	γ_2 C-C-C _{chain}
160		-	148	148	117	117	A _u	γ_3 C-C-C _{chain}
		-	142	142	143	143	A _u	δ Cl-Pd-Cl
		-	140	140	142	142	A _g	δ Cl-Pd-Cl
		-	127	127	110	110	A _g	γ_4 C-C-C _{chain}
117		-	121	121	167	167	A _u	τ C-N _{ring}
103		-	104	104	155	155	A _g	γ_5 C-C-C _{chain}
		-	89	89	80	80	A _u	γ N-Pd-Cl
		-	88	88	42	42	A _g	γ N-Pd-Cl
		-	75	75	73	73	A _u	γ' N-Pd-Cl
		-	74	74	71	71	A _g	γ' N-Pd-Cl
		-	70	70	111	111	A _u	Skeletal modes
		-	52	52	98	98	A _g	Skeletal modes
30		-	32	32	31	31	A _u	Skeletal modes
25		-	26	26	26	26	A _g	Skeletal modes
		-	23	23	23	23	A _u	Skeletal modes
		-	11	11	6	6	A _u	Skeletal modes

^aWavenumbers above 700 cm⁻¹ were scaled by 0.9499, accordingly to Merrick *et al.*³⁸ ^bWavenumbers scaled by 3 different scaling factors $\lambda_1=0.93$, $\lambda_2=1.01$ and $\lambda_3=1.11$ where λ_1 — ν NH₃, δ_{as} NH₃, ν Pd-Cl, δ N-Pd-N; λ_2 — δ_s NH₃, ρ NH₃, γ N-Pd-Cl; λ_3 — ν Pd-N, δ N-Pd-Cl, according to Fiuza *et al.*¹⁷ ^c ν = stretching; δ , β = in-plane deformation; ρ = rocking; τ = torsion; γ and γ' = in phase and out of phase out-of-plane deformation, respectively.

TABLE 4: Calculated (mPW1PW/LANL2DZ/6-31G*) scaling factors for selected vibrational modes, regarding different Pd(II)-amine complexes.

Compound	Scaling factor for each vibrational mode		
	$\nu\text{NH}_3/\nu\text{NH}_2$	$\nu\text{Pd-N}$	$\nu\text{Pd-Cl}$
cDDPd	0.91	1.13	0.93
[Pd(NH ₃) ₄] \cdot 2Cl \cdot H ₂ O	0.93	1.10	–
[Pd(NH ₃) ₃ (DMSO)] \cdot 2Cl	0.92	1.11	–
[PdCl ₂ (en)]	0.91	1.07	0.90
[PdCl ₂ (dap)]	0.92	1.20	0.89
[Pd ₂ -Spm]	0.92	1.17	0.94
Average	0.92	1.13	0.92